Hindawi
International Transactions on Electrical Energy Systems
Volume 2022, Article ID 4331293, 16 pages
https://doi.org/10.1155/2022/4331293

Research Article

Robust Allocation of FACTS Devices in Coordinated Transmission and Generation Expansion Planning considering Renewable Resources and Demand Response Programs

Sara Mahmoudi Rashid,[1] Ehsan Akbari,[2] Farshad Khalafian,[3] Mohmmad Hossein Atazadegan,[4] Saeid Shahmoradi,[5] and Abbas Zare Ghaleh Seyyedi[6]

[1]*Faculty of Electrical and Computer Engineering, University of Tabriz, Tabriz, Iran*
[2]*Department of Electrical Engineering, Mazandaran University of Science and Technology, Babol, Iran*
[3]*Department of Electrical Engineering, Ahvaz Branch, Islamic Azad University, Ahvaz, Iran*
[4]*Department of Electrical Engineering, Lorestan University, Khorramabad, Iran*
[5]*Khuzestan Water and Power Authority (KWPA), Ahvaz, Iran*
[6]*Department of Electrical Engineering, Shahid Bahonar University of Kerman, Kerman, Iran*

Correspondence should be addressed to Abbas Zare Ghaleh Seyyedi; abbas.zare.1990@gmail.com

Received 14 May 2022; Accepted 9 September 2022; Published 30 October 2022

Academic Editor: Pawan Sharma

Copyright © 2022 Sara Mahmoudi Rashid et al. This is an open access article distributed under the Creative Commons Attribution License, which permits unrestricted use, distribution, and reproduction in any medium, provided the original work is properly cited.

Nowadays, the use of demand response programs (DRPs) in a variety of long-term and short-term planning problems has been explored. In this paper, a generation and transmission expansion planning (GTEP) model along with FACTS device allocation is presented. Furthermore, demand response programs are taken into account for more load flexibility. The proposed model is presented as a multi-objective minimizing problem considering emission, cost, and voltage security index. Furthermore, the conventional Pareto optimization is adopted using fuzzy weighted sum method (FWSM) to achieve a single-objective model. The final problem is constrained by equations of alternative current power flow, operation and voltage security limits, planning model of shunt FACTS devices, and operation of the DRP. Adaptive robust optimization (ARO) is used to reach suitable models for the active power of renewable resources and power consumption. As a main search algorithm, a hybrid combination of water cycle algorithm (WCA) and ant lion optimization (ALO) is proposed to find the optimum solution with a small standard deviation. The problem is tested on different standard IEEE systems, and the results validate the operation and network security improvement due to optimal location of FACTS devices. According to the results, the economic and environmental status of the network has also improved.

1. Introduction

Among the development and expansion solutions to power systems is generation and transmission expansion planning (GTEP), which helps optimize the sitting and sizing of sources and lines, thus supplying the future energy demands [1]. This can be realized considering various technical, economic, and environmental objectives [2]. To overcome the high cost of operation and considerably high pollution levels and reduce them to the least amounts as much as possible, the electricity industry tries to utilize renewable energy sources (RESs) [3], more specifically wind turbines (WTs) [4]. Since the output power of renewable sources is uncertain and intermittent, the operation will vary every day and hour; hence, there will be unbalanced electricity throughout the system, and the cost of RESs will rise because of unbalanced operation [5]. This discussion is mostly interrelated with the reduced flexibility of the system, which can be realized by adopting flexible sources such as DRP and battery storage banks [6]. The GTEP should be done to meet the high energy demand and electricity consumption surges at peak-load circumstances such as holidays when voltage

collapses are highly likely. One solution is to advise and take action beforehand [7]. By utilizing suitable models for GTEP, the abovementioned objectives can be satisfied.

Expansion planning methods for the power grids have widely been introduced in the literature. An adaptive robust model for GTEP is used in [8] in a system that includes wind turbines. Since the system energy demand is uncertain, storage systems, dynamic thermal rating systems, and optimum line switching approaches have been used to make the power system's response flexible. The model is subject to technical and economic constraints on uncertainty parameters. In an attempt to reduce the capital and operating cost, a stochastic co-optimization planning strategy is used [9], in which a linearized model-based AC power flow maintains the bus voltages, reactive power, and active power loss of the system. To compensate for reactive power, some equipment, including power generation sources, transmission lines, static var compensators (SVCs), and capacitor banks, was used in the same study. Moreover, the suggested model considers the loss of load expectation (LOLE). The authors in [10] discuss the GTEP problem subject to the vulnerability of the system in case of terrorist attacks and earthquakes. By doing this, the system will be reliable and safe for future operations.

One generation expansion planning-unit commitment method was presented to upgrade the available models [11]. Investment decisions made on RESs, storage devices, and thermal equipment are optimized. The model also considers real-time flexibility. Expansion planning is also discussed based on a mixed-integer linear robust multiobjective strategy [12]. Taking uncertainty effect into account when dealing with the demand and price of system elements, the researchers also introduce a structure based on information-gap decision theory (IGDT). Reference [13] considers the impact of reliability parameters on expansion planning, in which value-at-risk (VaR) and conditional VaR (CVaR) are also adopted. This study uses Bender's decomposition to divide the planning problem to one investment problem and two subproblems. The aim is to assess the status of operating cost and reliability index. Thyristor-controlled series compensators (TCSCs) are used in [14] in the transmission expansion model to increase the line capacity. In addition, short-circuit level is controlled by using superconducting fault current limiters (SFCLs). TCSCs and SFCLs together help reach a suitable optimal expansion plan. Reference [15] enhances the transmission network operation using a constant series capacitor (CSC) along with DRP for the GTEP. The conventional formulae of GTEP are mixed-integer nonlinear programming (MINLP). But [13] adopts a linearized approximating method (LAM) based on direct current (DC) power flow equations. Linearized AC power flow equations based on LAM have also been used in expansion planning [14]. Nonhybrid evolutionary algorithms (NHEAs) are also used to deal with expansion planning [16].

Various uncertainties include the amount of load, the energy price, RES output power, and impact of power sources planning. As a robust model can find an optimal solution when dealing with uncertainty parameters, it has been discussed in many works. In a min–max framework for the problem, ARO was used for modeling the demand and RES output power uncertainties [17]. The max term specifies the worst scenario, while the min term finds its optimal solution. A max term for the suggested technique is found according to the dual theory [18]. The energy demand and price of energy, and of EVs as uncertainties can be expressed by the boundary uncertainty robust optimization (BURO) [19], where uncertainties are represented by integer values between the upper and lower boundaries of the uncertainty. The robust model based on a linear problem has also been incorporated in [19], while the ARO model works using a nonlinear problem [20]. Table 1 summarizes the studies in this specific area.

Some of the points worth taking into account in the planning of power systems are as follows:

(i) Security and pollution level are among the indices that need more focus in the GTEP of power systems. The optimality of an index does not necessarily guarantee the optimal status of another index. For instance, energy cost reduction equals higher power injection by power sources, hence occurrence of overvoltage and escalated loss. Thus, various effective indices need to be taken into account at the same time.

(ii) The GTEP is MINLP, and a LAM is used to solve it. Yet, LAM leads to considerable calculation errors. This is more sensible in cases where the GTEP is based on DC power flow. Moreover, this model cannot appropriately analyze voltage security, and implementation of reactive power planning is not possible. According to the linearized AC power flow, the calculation errors made in LAM for modeling the GTEP cannot be neglected [4]. Besides, the problem is solved using NHEAs, in which unique response conditions are not provided. To overcome this challenge, hybrid evolutionary algorithms (HEAs) are recommended, where decision variables are updated and unique approximate response conditions are met.

(iii) In general, stochastic and probabilistic programming has been used to model uncertainties. But to ensure the optimal solution is obtained, robust planning is a suitable method. This is because it determines an optimal point that is robust to uncertainties. In this topic, various research works have been presented in the literature. However, they generally used a robust model such as ARO and BURO that can only be presented on linear problems. Nevertheless, based on the second research gap, using the LAM for GTEP bears a significant computational error. While ARO is applied to a nonlinear problem in [20], it has complexities, including dual gap and complementarity (equilibrium) constraints. To compensate for this, a combination of ARO and HEA is expected to provide a suitable capability.

Table 1: Comparison of the proposed strategy with latest literature.

Ref.	Indices				Uncertainty model	Solver
	Economic status	Operation	Security	Environmental status		
[8]	Yes	Yes	No	No	ARO	LAM
[9]	Yes	Yes	No	No	Stochastic	LAM
[10]	Yes	Yes	No	No	Stochastic	NHEA
[11]	Yes	Yes	No	No	Stochastic	LAM
[12]	Yes	Yes	No	No	IGDT	LAM
[13]	Yes	Yes	No	No	Stochastic	LAM
[16]	Yes	Yes	No	No	Stochastic	NHEA
[17]	Yes	Yes	No	No	ARO	LAM
[19]	Yes	Yes	No	No	BURO	LAM
[20]	Yes	Yes	No	No	ARO	NMA
PS	Yes	Yes	Yes	Yes	HEA-based ARO	HEA

PS: proposed strategy, HEA: hybrid evolutionary algorithm, NMA: numerical mathematical approach.

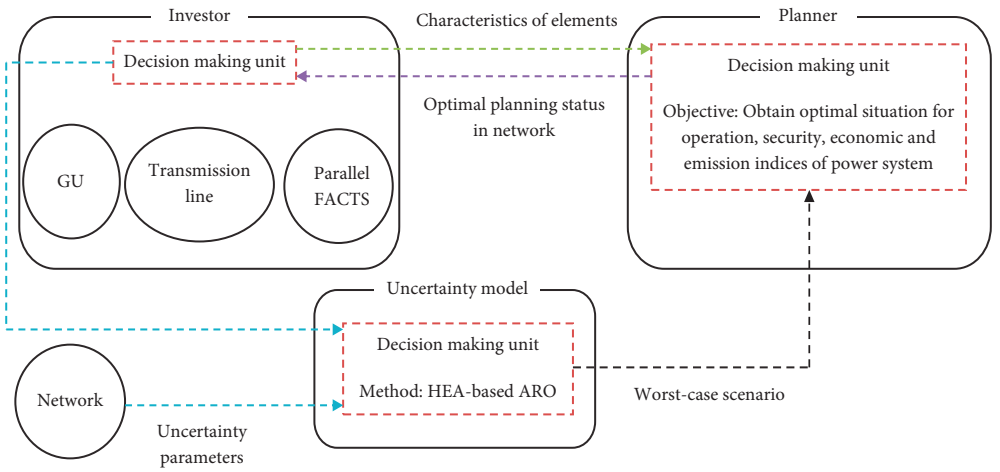

Figure 1: Proposed GTEP framework.

This paper attempts to fill the abovementioned gaps, Figure 1. The placement of shunt FACTs devices when dealing with the GTEP problem is also addressed to predict the optimal operation situation, voltage security, and economic and environmental indices. This strategy can be structured like three-objective optimization minimizing the cost of planning (which is the total capital cost of generation units and shunts FACTS devices, in addition to transmission lines together with generation units' operating cost), the pollution level released by generation units, and the index L_{max} (concerning voltage security). The Pareto optimization method based on the sum of weighted functions method is employed to structure the objective function. The function relies on operation limits, equations of AC power flow, security of voltage, DRP operation model, operation of shunt FACTS devices, and planning model. The best solution compromised among objective functions is specified using the fuzzy decision method. Moreover, the ARO is adopted to model the energy demand and active power of RESs suitably. The HEA based on hybrid WCA-ALO solves the problem and finds an optimal solution. Notable innovations presented in this paper include the following:

(i) Presenting a GTEP model to plan reactive power sources to supply reliable, clean energy.

(ii) Modeling operation, security, economic status, and environmental status indices at the same time.

(iii) Robustly modeling the demand and output power of renewables using the MINLP model of the GTEP by adopting the HEA-based ARO.

(iv) Adopting the hybrid WCA-ALO to find the optimum solution in the final response that has small standard deviation in special approximate response situations.

The rest of this paper is organized as follows. The GTEP formulation will be described in Section 2. The uncertainty modeling and the problem resolving procedure by the HEA-based ARO are presented in Section 3. Section 4 illustrates the obtained results. Finally, Section 5 summarizes the conclusion.

2. Multi-Objective GTEP Strategy

The GTEP model in this section explains how to improve technical and economic indices for loads in the transmission network. A three-objective optimization problem is formulated for achieving the objectives of minimizing planning costs, greenhouse gases, and L_{max} index of the voltage

security index (VSI). A mathematical model can be given for the aforementioned problem, set upon the AC optimal power flow (AC-OPF) constraints, security of voltage, and operating model of DRP, along with active/reactive resource formulae, as follows:

$$\min F = \omega_{Cost}\overbrace{\frac{1}{2}\cdot\sum_{n,b\in N} C_{nb}^{TL} y_{nb}^{TL} + \sum_{p\in PaF} C_{p}^{PaF} y_{p}^{PaF} + \sum_{u\in GU} C_{u}^{GU} y_{u}^{GU} + \sum_{\substack{t\in T\\ y\in Y}} 365\times CF\times \sum_{u\in GU}\left(a_u + b_u P_{uty}^{GU} + c_g\left(P_{uty}^{GU}\right)^2\right)}^{Cost} + \omega_{EM}\overbrace{\sum_{\substack{t\in T\\ y\in Y}} 365\times CF\times \sum_{u\in GU-WF}^{EM}\left(\chi_u P_{uty}^{GU} + \delta_u\right)} + \omega_{VSI}\overbrace{\sum_{\substack{t\in T\\ y\in Y}} 365\times CF\times \sum_{n\in PQ}\left(\left(L_{nty}^{r}\right)^2 + \left(L_{nty}^{im}\right)^2\right)}^{VSI} \tag{1}$$

$$\sum_{u\in G} C_{u}^{GU} y_{u}^{GU} \le \overline{C}^{GU}, \tag{2}$$

$$\sum_{p\in PaF} C_{p}^{PaF} y_{p}^{PaF} \le \overline{C}^{PaF}, \tag{3}$$

$$\frac{1}{2}\cdot\sum_{n,b\in N} C_{nb}^{TL} y_{nb}^{TL} \le \overline{C}^{TL}, \tag{4}$$

$$y_{nb}^{TL} = y_{bn}^{TL} \quad \forall n, b, \tag{5}$$

$$\sum_{u\in GU} A_{nu}^{GU} P_{uty}^{GU} - \sum_{b\in N} A_{nb}^{TL} P_{nbty}^{TL} = \sum_{d\in D} A_{n\,d}^{D}\left(P_{dt\,y}^{D} - P_{dt\,y}^{DR}\right), \quad \forall n, t, y, \tag{6}$$

$$\sum_{u\in GU} A_{nu}^{GU} Q_{uty}^{GU} + \sum_{p\in PaF} A_{np}^{PaF} Q_{pty}^{PaF} - \sum_{b\in N} A_{nb}^{TL} Q_{nbty}^{TL} = \sum_{d\in D} A_{n\,d}^{D} Q_{dt\,y}^{D}, \quad \forall n, t, y, \tag{7}$$

$$P_{nbty}^{TL} = \left\{G_{nb}^{TL}\left(V_{nty}\right)^2 - V_{nty}\times V_{bty}\left\{G_{nb}^{TL}\cos\left(\alpha_{nty} - \alpha_{bty}\right) + B_{nb}^{TL}\sin\left(\alpha_{nty} - \alpha_{bty}\right)\right\}\right\} y_{nb}^{TL}, \quad \forall n, b, t, y, \tag{8}$$

$$Q_{nbty}^{TL} = \left\{-\left(B_{nb}^{TL} + \frac{B_{nb}^{TL0}}{2}\right)\left(V_{nty}\right)^2 - V_{nty}\times V_{bty}\left\{G_{nb}^{TL}\sin\left(\alpha_{nty} - \alpha_{bty}\right) - B_{nb}^{TL}\cos\left(\alpha_{nty} - \alpha_{bty}\right)\right\}\right\} y_{nb}^{TL}, \quad \forall n, b, t, y, \tag{9}$$

$$\underline{P}_{u}^{GU} y_{u}^{GU} \le P_{uty}^{GU} \le \overline{P}_{u}^{GU} y_{u}^{GU} \quad \forall u \in GU - WF, t, y, \tag{10}$$

$$\underline{Q}_{u}^{GU} y_{u}^{GU} \le Q_{uty}^{GU} \le \overline{Q}_{u}^{GU} y_{u}^{GU}, \quad \forall u, t, y, \tag{11}$$

$$P_{uty}^{GU} = \overline{P}_{uts}^{GU} y_u^{GU}, \quad \forall u \in WF, t, y, \tag{12}$$

$$-\overline{Q}_p^{PaF} y_p^{PaF} \le Q_{pty}^{PaF} \le \overline{Q}_p^{PaF} y_p^{PaF}, \quad \forall p, t, y, \tag{13}$$

$$-\beta_d P_{dt\ y}^{D} \le P_{dt\ y}^{DR} \le \beta_d P_{dt\ y}^{D}, \quad \forall d, t, y, \tag{14}$$

$$\sum_{t \in T} P_{dt\ y}^{DR} = 0, \quad \forall d, y, \tag{15}$$

$$\sqrt{\left(P_{nbty}^{TL}\right)^2 + \left(Q_{nbty}^{TL}\right)^2} \le \overline{S}_{nb}^{L}, \quad \forall n, b, t, y, \tag{16}$$

$$\underline{V}_n \le V_{nty} \le \overline{V}_n, \quad \forall n, t, y, \tag{17}$$

$$L_{nty}^{r} = 1 - \sum_{b \in PV} \frac{V_{bty}}{V_{nty}} \left(G_{nb}^{PQ-PV} \cos\left(\alpha_{nty} - \alpha_{bty}\right) - B_{nb}^{PQ-PV} \sin\left(\alpha_{nty} - \alpha_{bty}\right)\right), \quad \forall n \in PQ, t, y, \tag{18}$$

$$L_{nty}^{im} = -\sum_{b \in PV} \frac{V_{bty}}{V_{nty}} \left(G_{nb}^{PQ-PV} \sin\left(\alpha_{nty} - \alpha_{bty}\right) + B_{nb}^{PQ-PV} \cos\left(\alpha_{nty} - \alpha_{bty}\right)\right), \quad \forall n \in PQ, t, y. \tag{19}$$

subject to

Equation (1) specifies the objective functions of the suggested method. The first part of (1) includes minimizing planning cost of transmission lines in addition to the active/reactive resources. Costs for transmission lines, parallel FACTS, and GUs in the first and third terms are considered [1]. GUs' operating costs (fuel) are applied in the fourth term [4]. The transmission lines among *n*-*b* and *b*-*n* buses are similar, so a 1/2 factor is observed in the first section [1]. Equation (1) also addresses the environmental emission minimization (EM) resulting from the fossil fuel usage of nonrenewable GUs. Thus, it is not far-fetched that eco-friendly resources would take a larger portion of generation [21]. Equation (1), in its third part, tries to improve the situation of the network voltage security [22]. Here, $L_{\max}$ is used for grid security analysis, a numerical value that occurs between zero and one. No-load operation is indicated by a value of zero, and the voltage drop is indicated by a value of one. As a result, the third part of (1) requires the minimization of index L_{max} in order to ensure optimal voltage security.

The Pareto optimization method is used to formulate the objective function according to the summation of weighted functions [23]. Hence, various points are achieved for the values of $\omega_{VSI,}\omega_{EM,}\omega_{Cost}$ and parameters, for VSI, EM, and cost functions. The Pareto front of the suggested scheme is plotted in 3-dimensional coordination. Furthermore, the function has the lowest and highest values that could be computed through three cases provided by $\omega_{Cost} = 1$, $\omega_{EM} = 1$, and $\omega_{VSI} = 1$. To obtain the optimal compromise answer among the aforementioned functions, the fuzzy decision-making strategy can be applied. Detailed information is described as a fuzzy decision algorithm (Algorithm 1).

The planning model, including transmission lines, GUs, and parallel FACTSs, is considered in (2)–(5). Equations (2)–(4) show the investment budget equations for the GUs construction, parallel FACTSs, and transmission line,

respectively. Equation (5) indicates a logical limit which pursues the structure of transmission lines between n-b and b-n buses since both lines present identical transmission lines. The grid constraints of AC-PF are provided in (6)–(9) [1, 2], representing the balance between active and reactive power in the buses, along with availability of active/reactive power of transmission lines, respectively. Considering (8) and (9), when the binary variable of a transmission line presence (y^{TL}) is 1, it means that the line is joined to the grid; if not, it should be considered as disconnected.

In constraints (10)–(13), the planning and operation modeling of GUs and parallel FACTSs are given based on [1, 24], respectively. Equations (10) and (11) denote the GU generator ability curve that shows the real power production limitation (with positive value) in addition to GU controllable reactive power (which can have inductive and capacitive operation modes). It is worthy of note that (10) could be applied for nonrenewable GUs since renewable ones, like wind farms, because of small emissions and operation costs, typically (12), supply real power of the utmost capacity commensurate with weather condition to the grid [20]. For parallel FACTS operation or planning modeling, (13) shows the controllable reactive power limitation of the parallel FACTSs in both modes of inductive and capacitive operation. When the binary variables y^{GY} and y^{PaF} are equal to 1, GUs or parallel FACTSs will be connected to the network as shown in (10)–(13); if not, they will not be considered in the grid. Considering (14) and (15), the responsive load operation modeling is indicated [20]. Such loads are based on the incentive-based demand response programs (IDRP) [25]. As a result, these loads decrease their usage in peak times when the electricity price is high. In peak times, because of great usage of grid, GUs that have higher fuel costs can be estimated for playing part in power provision; hence, the local marginal price (LMP) is higher [21]. In addition, in off-peak times, cheap GUs provide electricity, consequently, the electricity costs get lower, and also the responsive loads consume lower electricity in peak times. Hence, based on this rule, (14) shows the load controllable power limitation of DRP plan; (15) states that the whole responsive load's decreased electricity in peak times can be obtained by grid [20].

Moreover, in (16) and (17) [21] and (18) and (19) [22], the transmission network technical constraints, namely, security and operation, are shown, respectively. The constraint related to the network operation, as shown in (16) and (17), respectively, refers to the apparent power limitation that flows in transmission lines and the boundary of bus voltage [20]. In (18) and (19), the network voltage security model is shown; it computes the $L_{\max}$ real and imaginary components in bus bars (PQ buses), respectively. It is worth mentioning that voltage-controlled bus (PV bus) has an assured distance from voltage drop point because of its capability of setting voltage. Therefore, $L_{\max}$ can be computed for PQ buses.

3. HEA-Based ARO Model for Suggested Design

3.1. Uncertainty Modeling. The suggested design in (1)–(19) includes uncertain variables like real and reactive loads, P^D and Q^D, and maximum WF real power, GU/P. In this study, in order to achieve a robust design for GTEP against the intermittent variables, the ARO is used for modeling the uncertainty noted in the suggested design. This model needs a scenario known as "*worst-case scenario*" [26]. The uncertainties in this scenario create the worst conditions for the problem, i.e., reducing the feasibility region. Therefore, the ARO is a suitable technique for modeling uncertainty and requires low computational efforts compared to probabilistic or stochastic programming [27]. Furthermore, WF would be uncertain because of the intermittent power generation. It is also predicted to be a proper resource to improve the operation, environmental emission, and voltage security indices of the transmission networks. Hence, robust modeling of its uncertainties obtains the robust ability of the WF to reach a network that consists of a proper technical situation. To put it differently, the response to the question "*Is the WF able to improve power system technical situation in the worst-case scenario?*" is given.

In the following, the matrix related to uncertainty parameters needed by ARO ($\overline{\vartheta}$) is introduced as (20), initially. According to this equation, the number of the rows should be equal to operational time number (n_t), and column number (n_c) is equal to $n_c = n_y(2n_d + n_u)$, where n_y, n_u, and n_d denote the numbers of planning years, WFs, and load blocks, respectively. In the ARO, the uncertainty variable (ϑ) is the true value of uncertainties. Hence, the uncertainty matrix variables for the matrix $\overline{\vartheta}$ are represented as (21). Afterward, according to [26], we need to determine the uncertainty set in the ARO method for the uncertainty variables, indicated for the t-th row of the matrix ϑ as (22).

$$\overline{\vartheta} = \left[P^D_{dt\ y|y=1} \cdots P^D_{dt\ y|y=n_y}\ Q^D_{dt\ y|y=1} \cdots Q^D_{dt\ y|y=n_y}\ \overline{P}^{GU}_{ut\,y|y=1} \cdots \overline{P}^{GU}_{ut\,y|y=n_y} \right]^T, \tag{20}$$

$$\vartheta = \left[P^{\vartheta}_{dt\ y|y=1} \cdots P^{\vartheta}_{dt\ y|y=n_y}\ Q^{\vartheta}_{dt\ y|y=1} \cdots Q^{\vartheta}_{dt\ y|y=n_y}\ \overline{P}^{\vartheta}_{ut\,y|y=1} \cdots \overline{P}^{\vartheta}_{ut\,y|y=n_y} \right]^T, \tag{21}$$

$$\Lambda_t^{\vartheta} = \left\{ \vartheta_t \in R^{n_c} : \frac{1}{n_c} \sum_{k=1}^{n_c} \frac{\left|\vartheta_{k,t} - \overline{\vartheta}_{k,t}\right|}{\widetilde{\vartheta}_{k,t}} \leq \Delta\vartheta, \quad \forall \vartheta_{k,t} \in \left[\overline{\vartheta}_{k,t} - \widetilde{\vartheta}_{k,t}, \overline{\vartheta}_{k,t} + \widetilde{\vartheta}_{k,t}\right] \right\} \forall t. \tag{22}$$

In (22), $\widetilde{\vartheta}$ indicates the uncertainty deviation, $\overline{\vartheta}$ is the predicted value of uncertainty, and $\Delta\vartheta$ denotes the uncertainty budget that is between zero and one. The zero value denotes the deterministic state of uncertainty ϑ, while the one value shows the worst-case scenario obtained by all the matrix elements (ϑ) [18]. Furthermore, the term $[\overline{\vartheta}_{k,t} - \widetilde{\vartheta}_{k,t}, \overline{\vartheta}_{k,t} + \widetilde{\vartheta}_{k,t}]$ indicates the changing amplitude of an uncertainty matrix element. Eventually, the uncertainties' set will be equal to unions Λ_t^{ϑ} as given in (50).

$$\Lambda^{\vartheta} = \bigcup_{t \in T} \Lambda_t^{\vartheta} \tag{23}$$

The *worst-case scenario* in the ARO method and its optimal value are obtained simultaneously [28]. In this method, it was observed that the worst state of the objective function belongs to the *worst-case scenario* compared with other scenarios. For instance, in minimizing the objective function of the main problem, a higher value would be achieved for the worst-case scenario compared with other scenarios. To mathematically model the problem, the term max is applied to the set of uncertainties in the main problem's objective function; hence, the true value of the uncertainty variable (ϑ) could be obtained. Thus, the uncertainty parameter ($\overline{\vartheta}$) could be replaced by the variable ϑ. Moreover, limitations of the robust problem based on the ARO would be identical to the constraints of the main problem and (23) [17]. As a result, the ARO-based robust model is described for the problem (1)–(19), as follows:

$$\begin{aligned} &\min_{y^{GU}, y^{TL}, y^{PaF}} \omega_{Cost} \left(\frac{1}{2} \cdot \sum_{n,b \in N} C_{nb}^{TL} y_{nb}^{TL} + \sum_{p \in PaF} C_p^{PaF} y_p^{PaF} + \sum_{u \in GU} C_u^{GU} y_u^{GU} \right) \\ &+ \min_z \max_{\vartheta} \omega_{Cost} \sum_{\substack{t \in T \\ y \in Y}} 365 \times CF \times \sum_{u \in GU} \left(a_u + b_u P_{uty}^{GU} + c_g \left(P_{uty}^{GU} \right)^2 \right) \\ &+ \omega_{EM} \sum_{\substack{t \in T \\ y \in Y}} 365 \times CF \times \sum_{u \in GU-WF} \left(\chi_u P_{uty}^{GU} + \delta_u \right) \\ &+ \omega_{VSI} \sum_{\substack{t \in T \\ y \in Y}} 365 \times CF \times \sum_{n \in PQ} \left(\left(L_{nty}^{r} \right)^2 + \left(L_{nty}^{im} \right)^2 \right), \end{aligned} \tag{24}$$

$$\text{constrained by equations (2) – (5),} \tag{25}$$

$$\text{equations (6) – (19), where the uncertainty variables of the matrix } \vartheta \text{ are replaced by uncertainty parameters of (20),} \tag{26}$$

$$\text{equation (23).} \tag{27}$$

It is worthy of mention that based on problem (1)–(19), the binary variables y^{TL}, y^{PaF}, and y^{GU} refer to the system construction status that is typically uncertainty independent and is frequent for the "*wait and see*" variable [17]. In contrast, "*here and now*" variables of the problem depend on uncertainty. Therefore, the term $\omega_{Cost}\,(1/2.\sum_{n,b\in N} C_{nb}^{TL} y_{nb}^{TL} + \sum_{p\in PaF} C_p^{PaF} y_p^{PaF} + \sum_{u\in GU} C_u^{GU} y_u^{GU})$in (1) and (2)–(5) is independent of uncertainty variables. Hence, the robust model's objective function (24) involves two sections: The first one includes merely min term since this part is independent of ϑ. The second part of (25), because of its dependency on uncertainty variables, contains min–max term. This part of the problem contains variable z that presents the vector of the continuous variables (1)–(19), namely, $L_{\max}$ real and imaginary components, voltage magnitude and angle of the network buses, and active/reactive power of different c. The term min in the second part of (24) is implemented for achieving the optimum value of z according to the main problem, (1)-(19), and the term max in this section achieves the uncertainty parameter values regarding the *worst-case scenario*. The equations of the problem in the robust model, (25)/(26), are similar to constraints (2)–(5)/(6)–(19); however, the variable ϑ is replaced with the parameter $\overline{\vartheta}$ in (26). The uncertainty set is the other constraint in ARO formulation (27), which refers to the permitted changing values of the variable ϑ.

3.2. Problem Solving according to the HEA. The suggested problem indicated in (24)–(27) is an MINLP problem. The dual model of this problem should be extracted for solving the problem using mathematical solvers until the min–max term changes to a max or min term. Nevertheless, the main formulation is hard to achieve and complicates the solution procedure because finding the dual model of an MINLP problem requires observing the duality gap equations and the equilibrium (complementarity) constraints [20]. Therefore, a linear anticipation formulation is initially achieved for the robust model of the optimization problem in most research works. Nevertheless, according to [4], this technique is accompanied by some computational errors, and computational errors for power losses in the linear AC-OPF problem are greater than ten percent in comparison with the nonlinear modeling of the distribution networks. Therefore, the solution achieved using this method consists of a small coefficient of reliability. To deal with the problem, this paper applies the HEA according to the hybrid algorithm based on WCA [29] and ALO [28] to obtain the optimum answer with a special response condition. The solver finds the optimum answer having the smallest error with the ultimate response because decision variables can be updated by both WCA and ALO procedures. Determination of the optimal compromised solution is given in subsection 4.1.b. The variables are divided into two groups for solving the suggested problem by the HEA algorithm: dependent and decision variables. The latter for the suggested scheme consists of y^{GU}, y^{PaF}, y^{TL}, and P^{GU} for nonrenewable GUs, Q^{GU}, P^{DR}, Q^{PaF}, and ϑ, and the values that can be designated by the hybrid ALO + WCA algorithm are commensurate with the following equations:

$$y_u^{GU} \in \{0,1\} \quad \forall u, \tag{28}$$

$$y_p^{PaF} \in \{0,1\} \quad \forall p, \tag{29}$$

$$y_{nb}^{TL} \in \{0,1\} \quad \forall n,b, \tag{30}$$

$$P_{uty}^{GU} \in \text{Equation}\,(10), \quad \forall u \in GU - WF, t, y, \tag{31}$$

$$Q_{uty}^{GU} \in \text{Equation}\,(11) \quad \forall u,t,y, \tag{32}$$

$$Q_{pty}^{PaF} \in \text{Equation}\,(13) \quad \forall p,t,y, \tag{33}$$

$$P_{dt\,y}^{DR} \in \text{Equation}\,(14) \quad \forall d,t,y, \tag{34}$$

$$\vartheta \in \Lambda^{\vartheta}. \tag{35}$$

The values of dependent variables, including L^r, L^{im}, P^{TL}, Q^{TL}, V, α, and P^{GU} for renewable GUs, are defined according to (6)–(9), (12), and (18)–(19) and the amount of the decision variables. In the current section, firstly, P^{GU} for renewable GUs is computed according to (12). Afterward, the variables P^{TL}, Q^{TL}, V, and α are achieved through the power flow constraints (6)–(9). The Newton–Raphson method is used in this study for solving the power flow equations. Eventually, (18) and (19) are applied to, respectively, compute L^r and L^{im}. In addition, a penalty function is applied for anticipating GU investment budget limitations, parallel FACTSs, and transmission lines, (2)–(4); IDRP operation constraint, (15); and system operation constraint, (16) and (17). In this method, the penalty function of $a = b$ is denoted by $\lambda.(b - a)$ and that of $a \le b$ is described as $\mu\times\max(0, a - b)$ [30]. $\mu \ge 0$ and $\lambda \in (-\infty, +\infty)$ show Lagrange coefficients, where determinated and updated by ALO + WCA. Afterward, the fitness function (FF) equals the objective function aggregation of the original problem according to this technique and is identical to (36), (24), and the penalty function. Finally, the optimal amount of FF is reached based on decision values and dependent variables provided in the following equation:

$$
\begin{aligned}
FF = \min_{y^{GU}, y^{TL}, y^{PaF}} & \left\{ \omega_{Cost} \left(\frac{1}{2}. \sum_{n,b \in N} C_{nb}^{TL} y_{nb}^{TL} + \sum_{p \in PaF} C_{p}^{PaF} y_{p}^{PaF} + \sum_{u \in GU}^{F_1} C_{u}^{GU} y_{u}^{GU} \right) + \mu^{GU}. \max\left(0, \sum_{u \in G} C_{u}^{GU} y_{u}^{GU} - C^{-GU} \right) \right. \\
& \left. + \mu^{PaF}. \max\left(0, \sum_{p \in PaF} C_{p}^{PaF} y_{p}^{PaF} - C^{-PaF} \right) + \mu^{TL}. \max\left(0, \frac{1}{2}. \sum_{n,b \in N} C_{nb}^{TL} y_{nb}^{TL} - C^{-TL} \right) \right\} \\
& + \min_{z} \max_{\vartheta} \left\{ \begin{array}{l}
\omega_{Cost} \sum\limits_{\substack{t \in T \\ y \in Y}} 365 \times CF \times \sum\limits_{u \in GU}^{F_2} \left(a_u + b_u P_{uty}^{GU} + c_g \left(P_{uty}^{GU} \right)^2 \right) + \\
\omega_{EM} \sum\limits_{\substack{t \in T \\ y \in Y}} 365 \times CF \times \sum\limits_{u \in GU-WF} \left(\chi_u P_{uty}^{GU} + \delta_u \right) + \\
\omega_{VSI} \sum\limits_{\substack{t \in T \\ y \in Y}} 365 \times CF \times \sum\limits_{n \in PQ} \left(\left(L_{nty}^{r} \right)^2 + \left(L_{nty}^{im} \right)^2 \right) \\
+ \sum\limits_{\substack{d \in D \\ y \in Y}} \lambda_{dy}^{DR} \sum\limits_{t \in T} P_{dty}^{DR} + \sum\limits_{\substack{n,b \in N \\ t \in T \\ y \in Y}} \mu_{nbty}^{TL}. \max\left(0, \sqrt{\left(P_{nbty}^{TL} \right)^2 + \left(Q_{nbty}^{TL} \right)^2} - S_{nb}^{-L} \right) \\
+ \sum\limits_{\substack{n \in N \\ t \in T \\ y \in Y}} \left\{ \underline{\mu}_{nty}^{V}. \max\left(0, \underline{V}_n - V_{nty} \right) + \mu_{nty}^{-V}. \max\left(0, V_{nty} - V_n^{-} \right) \right\}
\end{array} \right\}.
\end{aligned}
\tag{36}
$$

It is important to mention that as long as the convergence is provided, solutions of problem will be obtained; if not, according to the optimal FF value along with ALO + WCA solver rule, the decision variables will be updated. Here, convergence conditions are affordable when iteration number $iter_{max}$ achieves its maximum. Hence, the process of HEA problem solving can be as follows:

(i) Generating initial population (initialization step): the hybrid ALO + WCA algorithm randomly produces N (size of the population) various values for Lagrange multipliers and decision variables commensurate with their allowable range.

(ii) Calculating dependent variables (2nd step): dependent variables are computed according to (6)–(9), (12), and (18)–(19) for every decision variable value. It is worth mentioning that, according to (24)–(26), for independent decision-making variables, i.e., y^{GU}, y^{PaF}, and y^{TL}, all N values of the uncertainty variable, ϑ, are tested. Furthermore, all N decision variables for a value of ϑ, dependent on the uncertainty variable, i.e., P^{GU} for nonrenewable GUs, Q^{GU}, P^{DR}, Q^{PaF}, μ, and λ, are tested.

(iii) Determining the optimal value of FF (3rd step): the values F_1 and F_2 in (36) are reached for each decision variable value. Next, based on (36), the optimal FF value is equal to the summation of the minimum F_1 value and the minimum value of the maximizing F_2 for N decision variables.

(iv) Updating decision variables (4th step): the decision variable values are initially obtained based on the

ALO rule by optimal FF value. Then, they are updated by WCA rule. The FF and dependent variables are computed according to the 2nd and 3rd steps.

(v) Checking the convergency (5th step): by repeating the previous stage, $iter_{max}$ times, the convergence for the problem should be reached; otherwise, the 4th step should be iterated.

4. Numerical Results

Here, the suggested scheme is implemented on modified IEEE 6 and 89-bus grid. MATLAB software is used for simulations. Here, the uncertainty deviation ($\widetilde{\vartheta}$) is assumed to be the same amount for all intermittent parameters, which is considered as $r.\Delta\vartheta$, where r shows the uncertainty level. Next, the abilities of the noted strategies are implemented based on the numerical result achieved from various cases.

4.1. Modified IEEE 6-Bus Grid

4.1.1. Input Information. Figure 2 depicts the single-line illustration of this grid [1]. The initial voltage and power values are 230 kV and 100 MVA, respectively. The allowable voltage range is [0.5–1.05] p.u. According to the grid assumptions, it is possible to construct a line parallel to transmission lines. In [20], all current and candidate lines' specifications are provided, including construction cost, capacity, resistance, and reactance. It is possible to construct four renewable GUs of WF type and 13 nonrenewable GUs along with the presented GUs in the aforementioned grid. A1–A5 and B1–B8 show nonrenewable GUs and are, respectively, equipped in buses 1, 1, 2, 3, 6, 1, 2, 3, 6, 1, 1, 2, and 3. Moreover, W1 to W4 indicate wind farms that are, respectively, equipped in buses 6, 1, 1, and 2. All the existing and candidate GU specifications such as b factor in cost of the operation, construction cost, and emission coefficients are represented in [20]. In addition, [31] reported the maximum active power generation. 30% of $\frac{GU}{P}$ is presumed for the least and most GUs' reactive power, and the minimum output of active power is supposed to be 0. Furthermore, in the operation cost of GUs, the coefficients a and c are, respectively, presumed to be $10\times b$ and $10^{-4}\times b$. The daily real power profile of WFs can be obtained by multiplying their capacity by their daily power rate curve; this curve is represented in [1]. Furthermore, the consumption loads in buses 3–5 are 40%, 30%, and 30% of the total load of the grid. The planning horizon is considered for six years. For this horizon, the peak load of the network is 29–34 MW, with a coincidence coefficient of 70% and a power factor of 0.9. The hourly network load profile for a day is also equal to the load factor curve and generation of the annual peak load shown in [1]. Then, three parallel SVCs with the capacity of 5 MVA could be equipped in the network, which imposes \$10/kVAr/year construction cost [24]. Moreover, the investment budget of parallel FACTC, GUs, and transmission lines can be, respectively, presumed to be \$10 M, \$100 M, and \$20 M. Users would also have 30% contribution to DR program in this method.

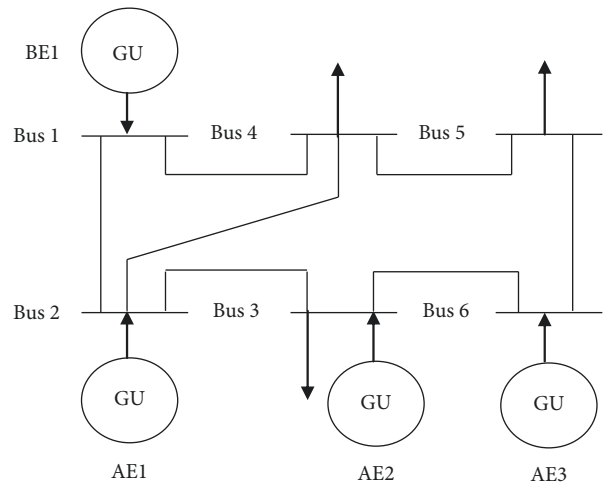

Figure 2: The modified 6-bus IEEE transmission grid [1].

4.1.2. Determination of the Optimal Compromise Solution. Table 2 presents the Pareto front of the suggested deterministic GTEP design using the fuzzy decision-making technique and the model denoted in (1)–(19). Table 2 lists the results of 0, 0.33, 0.5, and 1 of weighting coefficients, i.e., ωCost, ωEM, and ωVSI. Hence, based on Table 2 (or cases $\omega\text{Cost} = 1$, $\omega\text{EM} = 1$, $\omega\text{VSI} = 1$), changing range of the cost function is [91.8, 103.2] M\$. In addition, these intervals for VSI and EM functions are [20.9, 24.7] percent and [509, 673] tons, respectively. Furthermore, based on Table 2, the VSI, EM, and objective cost functions are not in the same directions. For instance, a decrease in VSI is proportional to a rise in planning cost since several GUs in the system are needed to enhance the voltage security of the network. It is equal to the increase in costs of planning and operation.

Table 3 reports the optimal solution compromises between the aforementioned objective functions achieved with ALO + WCA, ALO, WCA, crow search algorithm (CSA) [32], and grey wolf optimization (GWO) [33]. According to Table 3, the maximum convergence iteration number ($iter_{max}$) and the population size (N) for the aforementioned algorithms are considered 5000 and 80, respectively. The quality of the responses for the mentioned algorithms is defined by computing statistical indices like standard deviation (STD). In this regard, the solvers repeated the problem solution for 30 iterations. Table 3 reports the results for an uncertainty budget of 1 and various uncertainty levels. Eventually, the ALO + WCA algorithm gives the optimal solution compared with NHEAs, namely, CSA, GWO, WCA, and ALO. The optimal solution consists of the least VSI, EM, and cost values. For the computational time (CT) of 6.2 minutes in deterministic model ($\Delta\vartheta = 1$, $r = 0$), 711 was recorded for the least convergence iteration (CI) number. Additionally, compared with other algorithms, it has the minimum STD for this model (0.96%), which shows its low dispersion of the suggested GTEP problem ultimate solution. The VSI, EM, and cost values will be increased by raising (reducing) the load (WF production power) in robust modeling by increment in r of the worst scenario considering the scenario utilized in the deterministic model.

The best Pareto front compromise answer;
Optimum solution of Pareto and the decision-maker favors;
Step 1: Fuzzy membership function calculation
Values′ computation of the linear fuzzy membership function ($\widehat{F}_i$) of any Pareto optimum front member:
for i = Cost, EM, VSI
  if $F_i \le F_i^{\min}$
    The fuzzy membership function is noted as 1;
  elseif Fimin $\le F_i \le F_i^{\max}$
    it is considered as $F_i - F_i^{\max}/F_i^{\min} - F_i^{\max}$;
  elseif $F_i \ge F_i^{\max}$
    it is assumed as 0;
  end
end
Step 2: Obtain φm
$\varphi_m = \min(\hat{F}{}^m_{Cost}, \hat{F}{}^m_{EM}, \hat{F}{}^m_{VSI}) \quad \forall m \in \{1, 2, \ldots, n_m\}$, where m is a member of the Pareto front, n_m is total members.
Step 3: The best compromise answer
The best compromise answer is found via calculating $\max_m \ \varphi_m$

Algorithm 1: Pseudocode of the fuzzy decision support system.

Table 2: Pareto front of the suggested deterministic GTEP strategy.

ω_{Cost}	ω_{EM}	ω_{VSI}	Cost (10^6\$)	EM (ton)	VSI (%)
1	0	0	91.8	604	24.7
0	1	0	99.9	509	23.9
0	0	1	103.2	673	20.9
0.5	0.5	0	97.3	536	24.1
0.5	0	0.5	98.5	670	21.8
0	0.5	0.5	102.9	552	21.7
0.33	0.33	0.33	98.1	578	22.1

Furthermore, because of the decrease in the feasibility region of the suggested GTEP, the values of CT and CI increase in this condition. While SD value is almost the same with case of $\Delta\vartheta = 1$, $r = 0$, this is not true in NHEAs. Accordingly, the solution deviation reached by ALO + WCA could be indented from the feasibility region of the problem. Hence, the ALO + WCA solver approximates unique solution conditions, which aligns with the paper's second contribution noted in Section 1. In addition, the distance between the functions and the corresponding least values is lower in the optimal solution. Therefore, in the compromising point, the cost function obtains 36% ((95.9–91.8)/(103.2–91.8)) far from its lowest value, that is, \$91.8 M, in the deterministic model. In case of $\Delta\vartheta = 1$, $r = 0$, the values achieved are about 18.5% and 16% for VSI and EM functions, respectively.

4.1.3. Evaluating the Results of Network Expansion Planning. The results of the mentioned grid expansion planning related to the suggested robust and deterministic GTEP strategies by an uncertainty budget of 1 are reported in Table 4. Based on Table 4, three lines, T2, T6, and T7, are connected to the grid of Figure 2 for the two mentioned models. These lines are placed between buses 2 and 3, 5 and 6, and 3 and 6, respectively. In addition, for minimizing the environmental emission, planning cost, and $L_{\max}$ of security of voltage, every wind farm, W1–W4, in addition to units A1, A4, B5, B7, and B8, should be linked to the grid for various uncertainty levels provided in Table 4. Equation (1) presents the selection corresponding to the objective function. Then, at the bus bars of the network, three SVCs are installed at buses 3–5, for all uncertainty values, because installing SVCs in these buses helps to reduce the consumers' reactive consumption, and the voltage safety margin because of high X/R ratio of transmission grid is notably associated with the reactive power consumption. Hence, it is predicted that SCVs have amending effect on the security of voltage. They can also decrease losses of energy via line flow reduction and finally reduction in operation costs and emissions produced by GUs.

It is noteworthy that transmission line, SVC, and GU planning results are the same for both fixed and robust models (in the budget of uncertainty of one and different uncertainty levels). This is due to the construction status variable of the mentioned elements according to model (24)–(27), which does not depend on the decision variables; therefore, the same planning results are obtained for different levels of uncertainty. However, increasing the level of uncertainty compared to the definite model ($\Delta\vartheta = 1$, $r = 0$) results in GU operation cost increment and ultimately increases the total planning cost of the network. According to Table 4, the amount of active and reactive load in the worst scenario rises due to the increase in the uncertainty value

Table 3: The best compromise solution obtained by various algorithms in distinct robust model.

			$\Delta\vartheta = 1,\ r = 0$				
Algorithm	ω_{Cost}, ω_{EM}, ω_{VSI}	Cost (10^6 \$)	EM (ton)	VSI (%)	CI	CT (min)	SD (%)
ALO + WCA	0.38, 0.19, 0.43	95.9	535	21.6	711	6.2	0.964
ALO	0.38, 0.19, 0.43	97.3	551	22.8	967	7.5	1.73
WCA	0.38, 0.19, 0.43	97.6	558	23.1	1021	8.1	2.08
GWO	0.39, 0.20, 0.41	100.4	579	24.7	1437	9.4	2.94
CSA	0.39, 0.18, 0.43	101.7	591	25.5	1587	10.5	3.57
			$\Delta\vartheta = 1,\ r = 0.1$				
Algorithm	ω_{Cost}, ω_{EM}, ω_{VSI}	Cost (M\$)	EM (ton)	VSI (%)	CI	CT (min)	SD (%)
ALO + WCA	0.40, 0.20, 0.40	100.3	579	22.9	768	7.1	0.966
ALO	0.40, 0.20, 0.40	102.4	610	24.4	1093	9.2	2.09
WCA	0.40, 0.20, 0.40	103.0	621	24.9	1192	10	2.66
GWO	0.41, 0.21, 0.38	107.2	649	26.8	1611	11.9	3.55
CSA	0.39, 0.20, 0.41	109.3	666	27.9	1769	13.5	4.02

compared to the definite model-based scenario, but the level of active power generated by WFs decreases. Therefore, the demand for energy from GUs has increased in these conditions, leading to increment in costs of GU operation and total planning of the network. In addition, it can be observed from Table 4 that an increase in the level of uncertainty to 0.21 results in changes in the active and reactive loads and WF real power output in the worst-case scenario. However, the obtained results for $r > 0.21$ are the same as the results for $r = 0.21$. This value of r is known as the maximum level of uncertainty ($r_{\max}$) in this paper. This also means that the developed network is able to cover up to 21% of the prediction error of load uncertainties and active power generation of WFs. Suppose the prediction error of the mentioned uncertainties is more than 21%. In that case, it is expected that the planning results obtained in Table 4 for the mentioned network could not be successful in operation.

4.1.4. Examining the Abilities of the Suggested Method. To test the suggested method, five case studies can be proposed as follows:

(i) Analysis of load flow.

(ii) GTEP method neglecting DRP and SVC attribution.

(iii) GTEP method by SVC attribution.

(iv) GTEP method by DRP.

(v) GTEP Method by Both DRP and SVC Attribution.

Table 5 shows the environmental status, economic status, voltage security, and operation results for the mentioned grid with an uncertainty budget of 1 and various uncertainty values. The operation indices include total energy losses (TEL) over the planning period and maximum voltage deviation (MVD). According to this table, the cost is minimal in Case I, but it merely indicates the grid power flow results. Therefore, the cost function equals the AE1–AE3 and BE1 operation costs. Moreover, the grid and resources' technical limits are not taken into account in Case I; hence, it cannot be guaranteed that the mentioned sources will ensure consumption growth in the upcoming years. The results in Case II can be examined to prove this statement. In Case II, by considering the technical parameters, namely, power source, economic status, environmental status, voltage security, and operation limitations, it was seen that various resources and lines should be applied to the grid for fulfilling the consumption increase in the years ahead. With regard to SVC attribution and conducting the DR program in GTEP (Case V), the cost of planning is decreased according to Table 5by almost 16.8% ((115.3–95.9)/115.3) compared with Case II in the deterministic model ($r = 0$). In addition, Case V could decrease environmental emissions and voltage security by approximately 65.1% and 51.6%, respectively, compared with Case I in $r = 0$. In Case I, the highest TEL and MVD occur. Nevertheless, these parameters are improved in Case V by approximately 17.6% and 30.5%, in comparison with Case I in $r = 0$. Based on Table 5, the DR program strategy owns a considerable capability to decrease VSI, EM, and cost function in comparison with Case II. Furthermore, the DR program can also considerably influence the enhancement of MVD and TEL more than Case II. Hence, managing or storing the consumption would improve the environmental and economic conditions, grid voltage security, and operation indices. The SVC assignment can also potentially improve the security of voltage compared with Case II, and it has a significant impact on the improvement of the MVD status; however, the decrease of planning costs, TEL, and emissions is not considerable since these functions are less reactive power dependent. Nevertheless, the system voltage and VSI highly depend on reactive power because of the transmission grid high X/R ratio [22].

The results of the mentioned indicators for the maximum level of uncertainty and for different study cases are examined in Table 5. According to the table, an increase in the level of uncertainty in the worst-case scenario, in comparison with the strategy definite model-based scenario ($r = 0$), leads to an increase in cost, EM, VSI, TEL, and MVD parameters and finally results in the deterioration of economic status, environmental status, security, and network performance indicators of the model. These conditions are because of an increment of load and decrease of active generation capacity of WFs in the worst-case scenario, according to Table 4. In addition, it should be noted that the proposed design for V is able to cover the high prediction error of wind and load and production capacity compared to

Table 4: Planning results based on the suggested GTEP method in various uncertainty values of $\Delta\vartheta = 1$.

Model		Deterministic	Robust			
Uncertainty level (%)		0	0.1	$r_{max} = 0.21$	0.22	0.3
Max of P^D (p.u.)		34	37.4	39.8	39.8	39.8
Max of Q^D (p.u.)		16.5	18.15	19.15	19.15	19.15
Max of power rate of WF (p.u.)		1	0.9	0.82	0.82	0.82
Constructed transmission lines				T2, T6, T7		
Constructed GUs				A1, A4, B5, B7, B8, W1–W4		
Constructed SVCs				SVCs in buses 3–5		
Cost (10^6 \$)	Line investment			10.8		
	GUs investment			58.4		
	GUs operation	23.7	28.1	31.3	31.3	31.3
	GUs investment			3		
	Total	95.9	100.3	103.5	103.5	103.5

Table 5: Values of technical and economic indices for different uncertainty levels in $\Delta\vartheta = 1$.

R	0					r_{max}				
Case	I	II	III	IV	V	I	II	III	IV	V
r_{max}	—	—	—	—	—	0.09	0.17	0.18	0.20	0.21
Cost (10^6\$)	43.8	115.3	114.2	97.8	95.9	47.8	124.1	122.4	105.7	103.5
EM (ton)	1533	723	712	566	535	1671	831	818	662	626
VSI (%)	44.6	32.5	28.3	24.1	21.6	48.2	35.6	31.2	26.6	23.7
TEL (MWh)	31394	27471	27123	26263	25871	34210	31591	31191	30727	30269
MVD (p.u.)	0.059	0.053	0.045	0.043	0.041	0.061	0.056	0.048	0.046	0.044

other studies. Therefore, the suggested design can obtain more optimum values for the various mentioned indicators compared to cases I–IV, as well as in the case of forecast error or uncertainty of load and production capacity of WFs compared to cases. Other studies are more robust.

4.2. IEEE 89-Bus Grid. This grid has 35 bus bars, 12 nonrenewable GUs, and 210 transmission lines; their characteristics are reported in [34]. Maximum and minimum value of voltage are considered to be 1.05 and 0.95 p.u., respectively [35]. A new line can be paralleled with each transmission line, having similar specifications; this would be true for GUs. Furthermore, in buses 25, 28, 43, 67, and 83, 5 wind farms (W1–W5) with 200 MVA capacity are considered. The STATCOM type paralleled FACTS with 50 MVA capacity is considered in buses 13, 19, 31, 38–42, 60, 71, 81, and 89. Moreover, 5728 (1375), 6831 (1504), and 7942 (1654) MW (MVAr) are active (reactive) peak loads of 3 two-year periods. Transmission lines, GUs, and FACTs related investment budget is 100 times the investment budget of Section 4.1. Eventually, other characteristics like power factor of network, daily power rate curve of WF, *CP*, and other components, according to the information provided in Section 4.1, are assumed.

Table 6 and Figure 3 represent results of this section. Table 6 indicates the planning results of understudied grid for various uncertainty levels in $\Delta\vartheta = 1$. According to it, 5 WFs, 4 nonrenewable GUs, 16 transmission lines, and 12 STATCOMSs ought to be considered in the planning horizon for fulfilling the consumption increase in years ahead. The placement of STATCOMs and WFs is represented in the prior paragraph; however, the constructed transmission line and nonrenewable GU reports are presented in Table 6, and their information can be found in [17]. The planning consists of costs of construction of transmission lines, GUs, and STATCOMs, being \$197 M, \$1,045 M, and \$61 M, which are fixed for various uncertainty levels (r) since the binary variables corresponding to the constructed state of these elements are not dependent on uncertainty parameters. Nevertheless, the expected operation cost of GUs rises with the increase in r because the value of load (WFs active power) increases (reduces) compared to the deterministic model ($r = 0$), as shown in Table 4. On the other hand, according to the results of Table 6, the proposed design has a maximum uncertainty of 0.17; hence, this scheme in the network can have robust operation against the error of load uncertainty prediction and an active power of WFs up to 17%. Based on Table 6, the ALO + WCS algorithm can find the optimum solution of GTEP in the IEEE 89-bus network in convergence iteration (computational time) less than 1860 (18 minutes), with a final solution deviation similar to the results of the previous section, around 0.96%.

In Figure 3, the environmental emission, security, and operation (TEL and MVD) indices in Case I and Case V are reported for uncertainty budget one and different uncertainty levels. According to this figure, the EM and VSI functions are improved by the suggested GTEP method (Case V) considering the power flow analysis (Case I) in the different uncertainty levels by about 42.7% (12526726–71812)/125267) and 51.7%, respectively, in the deterministic model ($r = 0$). Operation indices like TEL and MDV are likewise enhanced by almost 33.4% and 29.8% in the aforementioned situations ($r = 0$), respectively.

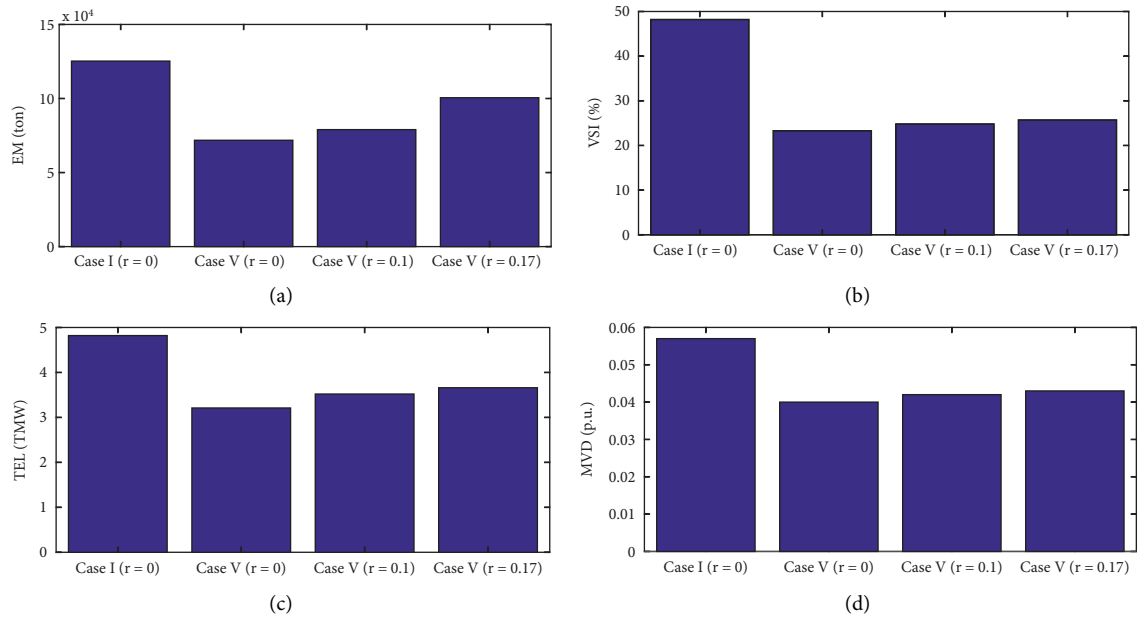

Figure 3: Values of technical indices for the different uncertainty levels and $\Delta\vartheta = 1$: (a) EM; (b) VSI; (c) TEL; (d) MVD.

Table 6: Planning, economic status, and convergence results for the different uncertainty levels and $\Delta\vartheta = 1$.

r		0	0.1	$r_{max} = 0.17$
Constructed transmission lines		T11, T17, T18, T31, T41, T55, T84, T98, T122, T139, T156, T169, T178, T179, T200, T208		
Constructed GUs		G3, G8, G9, G12, W1–W5		
Constructed STATCOMs		STATCOMs in buses 13, 19, 31, 38–42, 60, 71, 81, and 89		
Cost (10^6)	Transmission line investment	197		
	GUs investment	1045		
	GUs operation	482	531	555
	STATCOMs investment	61		
	Total	1785	1834	1858
CI		2107	2343	2512
CT (min)		15.1	16.7	18.0
SD (%)		0.965	0.966	0.967

According to Figure 3, as uncertainty value increases, theses indices increase compared to the case $r = 0$ because it raises (decreases) the load (active power of WFs) compared to the definite model according to Table 4.

5. Conclusion

tA GTEP model with parallel FACTS attribution is presented here for transmission grid and responsive loads. The proposed problem is three-objective optimization whose functions are minimizing planning costs, reducing non-renewable GU emissions, and minimizing the L_{max} of voltage security; model of parallel FACTS planning, security of voltage, operation, AC power flow relations, and operation model of DRP are constraints. The formulation is done according to the Pareto optimization method, which is based on the sum of the weighted functions method, to obtain a single-objective model for the suggested design. Moreover, the ARO is employed for modeling load uncertainties and real power from renewable resources. Next, to obtain the optimum solution, the hybrid ALO + WCA algorithm is applied. Eventually, based on presented results, this algorithm is able to gain the best compromise answer rather than NHEAs with the least computational time and convergence iteration number and with a standard deviation of approximately 0.96%. In other words, it is able to achieve unique solution's approximate conditions. With optimum placement of transmission lines, GUs, and paralleled FACTSs, the suggested GTEP strategy improved environmental status, security of voltage, losses of energy, and profiles of voltage by more than 42%, 51%, 18%, and 30%, respectively, based on optimum planning paid cost in comparison with power flow analysis. In addition, the uncertainty level increase of the solid model increases the load and decreases the active generation power of WFs in the worst-case scenario in comparison with the

deterministic model-based scenario. This also increases voltage drop, energy losses, operation costs, environmental emissions, and voltage safety index. But considering these cases, the proposed plan is able to find the optimum solution in the worst-case scenario so that it is able to cover the prediction error of uncertainty parameters between 17% and 21% for a specific planning result and obtain a robust solution.

Nomenclature

Indices and Sets

b:	Bus index
u, p, d, n, t, y:	Generation unit (GU), paralleled FACTS, load unit, bus, operation time, planning year related indices
GU, PaF, D, N, T, Y:	Sets of generation unit (GU), parallel FACTS, load block, bus, operation time, planning year
PQ, PV:	Sets of Bus bar (PQ bus) and voltage-controlled bus (PV bus)
WF:	Set of renewable GU buses.
*Variables*Cost, EM, VSI:	Cost, EM, VSI:Cost of planning ($), emission (ton), and voltage security index
L^r, L^{im}:	$L_{\max}$ real and imaginary components in voltage security
P^{DR}, P^{GU}, P^{TL}:	DRP, GU, and transmission line related active powers (p.u.)
P^{ϑ}, Q^{ϑ}, $\frac{\vartheta}{P}$:	Uncertainty variable of active and reactive load and renewable power (p.u.)
Q^{PaF}, Q^{GU}, Q^{TL}:	Reactive power of parallel FACTS, GU, and transmission line (p.u.)
V, α:	Voltage magnitude (p.u.) and angle (rad)
y^{PaF}, y^{TL}, y^{GU}:	Paralleled FACTS, transmission lines, and GU construction status; y^{PaF}, y^{TL}, $y^{GU} \in \{0, 1\}$.

Parameters

a, b, c:	Fuel cost equation coefficients for GU in $, $/MWh, and $/MWh^2, respectively
A^D, A^{PaF}, A^{TL}, A^{GU}:	Incidence matrix bus and load block, bus and parallel FACTS, bus and transmission line, bus and GU
CF:	Coincidence coefficient
C^{PaF}, C^{TL}, IC^{GU}:	Cost of construction of parallel FACTS, transmission line, and GU ($)
$\overline{C}^{PaF}$, $\overline{C}^{TL}$, $\overline{C}^{GU}$:	Maximum budget of investment for parallel FACTS, transmission line, and GU ($)
G^{PQ-PV}, B^{PQ-PV}:	Matrices of conductance and susceptance according to the link between PQ and PV buses (p.u.)
G^{TL}, B^{TL}, B^{TL0}:	Series conductance and susceptance, and parallel susceptance of a transmission line (p.u.)
P^D, Q^D:	Load active and reactive power (p.u.)
$\underline{P}^{GU}$, $\overline{P}^{GU}$:	Lower and upper value of GU active power (p.u.)
$\underline{Q}^{GU}$, $\overline{Q}^{GU}$:	GU reactive power's lower and upper limits (p.u.)
$\underline{Q}^{PaF}$, $\overline{Q}^{PaF}$:	Parallel FACTS reactive power's lower and upper limits (p.u.)
$\overline{S}^{TL}$:	Transmission line maximum capacity (p.u.)
$\underline{V}$, $\overline{V}$:	Voltage magnitude's lower and upper limits (p.u.)
β:	Participation rate of load block in the DRP
χ, δ:	Coefficients of emission equation for GU, respectively, in ton/MW and ton
ω_{Cost}, ω_{EM}, ω_{VSI}:	Weighed coefficients in objective function.

Data Availability

Data sharing not applicable. No new data were created or analyzed in this study.

Conflicts of Interest

The authors declare that they have no conflicts of interest.

References

[1] H. Hamidpour, S. Pirouzi, S. Safaee, M. Norouzi, and M. Lehtonen, "Multi-objective resilient-constrained generation and transmission expansion planning against natural disasters," *International Journal of Electrical Power & Energy Systems*, vol. 132, Article ID 107193, 2021.

[2] H. Eroğlu, E. Cuce, P. Mert Cuce, F. Gul, and A. Iskenderoğlu, "Harmonic problems in renewable and sustainable energy systems: a comprehensive review," *Sustainable Energy Technologies and Assessments*, vol. 48, Article ID 101566, 2021.

[3] L. Al-Ghussain, A. Darwish Ahmad, A. M. Abubaker, and M. A. Mohamed, "An integrated photovoltaic/wind/biomass and hybrid energy storage systems towards 100% renewable energy microgrids in university campuses," *Sustainable Energy Technologies and Assessments*, vol. 46, Article ID 101273, 2021.

[4] M. R. Ansari, S. Pirouzi, M. Kazemi, A. Naderipour, and M. Benbouzid, "Renewable generation and transmission expansion planning coordination with energy storage system: a flexibility point of view," *Applied Sciences*, vol. 11, no. 8, p. 3303, 2021.

[5] J. Aghaei, M. Barani, M. Shafie-khah, A. A. Sanchez de la Nieta, and J. P. S. Catalao, "Risk-constrained offering strategy for aggregated hybrid power plant including wind power producer and demand response provider," *IEEE Transactions on Sustainable Energy*, vol. 7, no. 2, pp. 513–525, 2016.

[6] M. Norouzi, J. Aghaei, S. Pirouzi, T. Niknam, and M. Lehtonen, "Flexible operation of grid-connected microgrid using ES," *IET Generation, Transmission & Distribution*, vol. 14, no. 2, pp. 254–264, 2019.

[7] S. R. Nandanwar, M. L. Kolhe, S. B. Warkad, N. P. Patidar, and V. K. Singh, "Voltage security assessment by using PFDT and CBR methods in emerging power system," *Energy Procedia*, vol. 144, pp. 170–181, 2018.

[8] S. Dehghan, N. Amjady, and P. Aristidou, "A robust coordinated expansion planning model for wind farm-integrated power systems with flexibility sources using affine policies," *IEEE Systems Journal*, vol. 14, no. 3, pp. 4110–4118, 2020.

[9] Z. Zhou, C. He, T. Liu et al., "Reliability-constrained AC power flow-based Co-optimization planning of generation and transmission systems with uncertainties," *IEEE Access*, vol. 8, pp. 194218–194227, 2020.

[10] M. Shivaie, M. Kiani-Moghaddam, and P. D. Weinsier, "A vulnerability-constrained quad-level model for coordination of generation and transmission expansion planning under seismic- and terrorist-induced events," *International Journal of Electrical Power & Energy Systems*, vol. 120, Article ID 105958, 2020.

[11] D. A. Tejada-Arango, G. Morales-Espana, S. Wogrin, and E. Centeno, "Power-based generation expansion planning for flexibility requirements," *IEEE Transactions on Power Systems*, vol. 35, no. 3, pp. 2012–2023, 2020.

[12] H. Mavalizadeh, A. Ahmadi, F. H. Gandoman, P. Siano, and H. A. Shayanfar, "Multiobjective robust power system expansion planning considering generation units retirement," *IEEE Systems Journal*, vol. 12, no. 3, pp. 2664–2675, 2018.

[13] L. C. da Costa, F. S. Thome, J. D. Garcia, and M. V. F. Pereira, "Reliability-constrained power system expansion planning: a stochastic risk-averse optimization approach," *IEEE Transactions on Power Systems*, vol. 36, no. 1, pp. 97–106, 2021.

[14] M. Esmaili, M. Ghamsari-Yazdel, N. Amjady, C. Y. Chung, and A. J. Conejo, "Transmission expansion planning including TCSCs and SFCLs: a MINLP approach," *IEEE Transactions on Power Systems*, vol. 35, no. 6, pp. 4396–4407, 2020.

[15] M. Zeinaddini-Meymand, M. Rashidinejad, A. Abdollahi, M. Pourakbari-Kasmaei, and M. Lehtonen, "A demand-side management-based model for G&TEP problem considering FSC allocation," *IEEE Systems Journal*, vol. 13, no. 3, pp. 3242–3253, 2019.

[16] P. Vilaça Gomes, J. T. Saraiva, L. Carvalho, B. Dias, and L. W. Oliveira, "Impact of decision-making models in Transmission Expansion Planning considering large shares of renewable energy sources," *Electric Power Systems Research*, vol. 174, Article ID 105852, 2019.

[17] H. Kiani, K. Hesami, A. Azarhooshang, S. Pirouzi, and S. Safaee, "Adaptive robust operation of the active distribution network including renewable and flexible sources," *Sustainable Energy, Grids and Networks*, vol. 26, Article ID 100476, 2021.

[18] S. Dehghan, N. Amjady, and A. Kazemi, "Two-stage robust generation expansion planning: a mixed integer linear programming model," *IEEE Transactions on Power Systems*, vol. 29, no. 2, pp. 584–597, 2014.

[19] A. Shahbazi, J. Aghaei, S. Pirouzi, M. Shafie-khah, and J. P. S. Catalão, "Hybrid stochastic/robust optimization model for resilient architecture of distribution networks against extreme weather conditions," *International Journal of Electrical Power & Energy Systems*, vol. 126, Article ID 106576, 2021.

[20] S. Pirouzi, J. Aghaei, M. A. Latify, G. R. Yousefi, and G. Mokryani, "A robust optimization approach for active and reactive power management in smart distribution networks using electric vehicles," *IEEE Systems Journal*, vol. 12, no. 3, pp. 2699–2710, 2018.

[21] H. Hamidpour, J. Aghaei, S. Dehghan, S. Pirouzi, and T. Niknam, "Integrated resource expansion planning of wind integrated power systems considering demand response programmes," *IET Renewable Power Generation*, vol. 13, no. 4, pp. 519–529, 2019.

[22] S. M. Mohseni-Bonab, A. Rabiee, and B. Mohammadi-Ivatloo, "Voltage stability constrained multi-objective optimal reactive power dispatch under load and wind power uncertainties: a stochastic approach," *Renewable Energy*, vol. 85, pp. 598–609, 2016.

[23] W. Jakob and C. Blume, "Pareto optimization or cascaded weighted sum: a comparison of concepts," *Algorithms*, vol. 7, no. 1, pp. 166–185, 2014.

[24] S. A. Eghbali Khob, M. Moazzami, and R. Hemmati, "Advanced model for joint generation and transmission expansion planning including reactive power and security constraints of the network integrated with wind turbine," *International Transactions on Electrical Energy Systems*, vol. 29, no. 4, p. e2799, 2018.

[25] P. Harsh and D. Das, "Energy management in microgrid using incentive-based demand response and reconfigured network considering uncertainties in renewable energy sources," *Sustainable Energy Technologies and Assessments*, vol. 46, Article ID 101225, 2021.

[26] Z.-Z. Wu, Y. P. Xu, Z. L. Cheng et al., "Optimal placement and sizing of the virtual power plant constrained to flexible-renewable energy proving in the smart distribution network," *Sustainable Energy Technologies and Assessments*, vol. 49, Article ID 101688, 2022.

[27] Z. Yang, M. Ghadamyari, H. Khorramdel et al., "Robust multi-objective optimal design of islanded hybrid system with renewable and diesel sources/stationary and mobile energy storage systems," *Renewable and Sustainable Energy Reviews*, vol. 148, Article ID 111295, 2021.

[28] M. Mani, O. Bozorg-Haddad, and X. Chu, *Ant Lion Optimizer (ALO) Algorithm," Advanced Optimization By Nature-Inspired Algorithms*, , pp. 105–116, Springer Singapore, 2017.

[29] A. Sadollah, H. Eskandar, H. M. Lee, D. G. Yoo, and J. H. Kim, "Water cycle algorithm: a detailed standard code," *Software*, vol. 5, pp. 37–43, 2016.

[30] W. K. A. Najy, H. H. Zeineldin, and W. L. Woon, "Optimal protection coordination for microgrids with grid-connected and islanded capability," *IEEE Transactions on Industrial Electronics*, vol. 60, no. 4, pp. 1668–1677, 2013.

[31] J. Aghaei, N. Amjady, A. Baharvandi, and M.-A. Akbari, "Generation and transmission expansion planning: MILP–based probabilistic model," *IEEE Transactions on Power Systems*, vol. 29, no. 4, pp. 1592–1601, 2014.

[32] A. Askarzadeh, "A novel metaheuristic method for solving constrained engineering optimization problems: crow search algorithm," *Computers & Structures*, vol. 169, pp. 1–12, 2016.

[33] A. Saxena, R. Kumar, and S. Mirjalili, "A harmonic estimator design with evolutionary operators equipped grey wolf optimizer," *Expert Systems with Applications*, vol. 145, Article ID 113125, 2020.

[34] T. Hussain, S. Suryanarayanan, T. M. Hansen, and S. M. S. Alam, *A Computationally Improved Heuristic Algorithm for Transmission Switching Using Line Flow Thresholds for Load Shed Reduction*, pp. 1–6, IEEE Madrid PowerTech, Madrid, Spain, 2021.

[35] S. Pirouzi, M. A. Latify, and G. R. Yousefi, "Investigation on Reactive Power Support Capability of PEVs in Distribution Network Operation," *23rd Iranian Conference on Electrical Engineering*, pp. 1591–1596, Tehran, Iran, May 2015.